Folding and Domain−Domain Interactions of the Chaperone PapD Measured by ^{19}F NMR†

James G. Bann*,‡ and Carl Frieden*

Department of Biochemistry and Molecular Biophysics, Washington University in St. Louis School of Medicine, 660 South Euclid Avenue, St. Louis, Missouri 63110

Received June 30, 2004; Revised Manuscript Received August 16, 2004

ABSTRACT: The folding of the two-domain bacterial chaperone PapD has been studied to develop an understanding of the relationship between individual domain folding and the formation of domain−domain interactions. PapD contains six phenylalanine residues, four in the N-terminal domain and two in the C-terminal domain. To examine the folding properties of PapD, the protein was both uniformly and site-specifically labeled with *p*-fluoro-phenylalanine (^{19}F-Phe) for ^{19}F NMR studies, in conjunction with those of circular dichroism and fluorescence. In equilibrium denaturation experiments monitored by ^{19}F NMR, the loss of ^{19}F-Phe native intensity for both the N- and C-terminal domains shows the same dependence on urea concentration. For the N-terminal domain the loss of native intensity is mirrored by the appearance of separate denatured resonances. For the C-terminal domain, which contains residues Phe 168 and Phe 205, intermediate as well as denatured resonances appear. These intermediate resonances persist at denaturant concentrations well beyond the loss of native resonance intensity and appear in kinetic refolding ^{19}F NMR experiments. In double-jump ^{19}F NMR experiments in which proline isomerization does not affect the refolding kinetics, the formation of domain−domain interactions is fast if the protein is denatured for only a short time. However, with increasing time of denaturation the native intensities of the N- and C-terminal domains decrease, and the denatured resonances of the N-terminal domain and the intermediate resonances of the C-terminal domain accumulate. The rate of loss of the N-terminal domain resonances is consistent with a cis to trans isomerization process, indicating that from an equilibrium denatured state the slow refolding of PapD is due to the trans to cis isomerization of one or both of the N-terminal cis proline residues. The data indicate that both the N- and C-terminal domains must fold into a native conformation prior to the formation of domain−domain interactions.

PapD is a chaperone required for the assembly of the subunits of P-pili in the periplasm of uropathogenic *Escherichia coli.* In the absence of PapD these subunits are proteolytically degraded (*1*). The protein is composed of two domains with each domain having an immunoglobulin (Ig)-like fold (Figure 1) (*2*). Previous experiments have shown that equilibrium denaturation in urea using fluorescence or circular dichroism (CD)[1] is a single cooperative transition, whereas experiments with 6-^{19}F-tryptophan (6-^{19}F-Trp) labeled protein using ^{19}F NMR show an intermediate form (*3*). This intermediate, originating from Trp 128 in the C-terminal domain, was characterized by an observable peak that resonated at a frequency between that of the native 6-^{19}F-Trp 128 and that of denatured 6-^{19}F-Trp 128 resonances. The intermediate appeared at urea concentrations from the start of the transition from native to denatured and persisted beyond the complete loss of native resonance intensity (*3*). Furthermore, the same intermediate was observed to form rapidly in the refolding kinetics as monitored by stopped-flow ^{19}F NMR, consistent with a rapid change in CD at 230 nm, and indicating the C-terminal domain forms structure before the N-terminal domain (*3*).

Because the chemical shift difference between the native and denatured resonances of 6-^{19}F-Trp 36 in the N-terminal domain was small and because Trp 36 is a surface-exposed residue, it was difficult to determine whether the N-terminal domain may also form an intermediate. We hypothesized previously that the slow rate of folding (accumulation of native N- and C-terminal domain resonances) was due to the slow trans to cis isomerization of one or both of two cis proline residues (Pro 49 and Pro 54) in the N-terminal domain. Until the trans to cis isomerization event occurred, the N-terminal domain could not fold and the formation of domain−domain interactions was prevented. An alternative hypothesis is that folding of the N-terminal domain is dependent on the C-terminal domain. In this case the intermediate would represent a misfolded form of the protein and must initially correct itself (which may be a slow process) in order to form domain−domain interactions. The rate-limiting step would then be the "correct" folding of the C-terminal domain, followed by the folding of the N-terminal domain and the subsequent formation of domain−domain interactions. The ^{19}F NMR data we presented earlier could not distinguish between these two possibilities.

† This work was supported by NIH Grant DK13332 (C.F.) and in part by a Keck fellowship to J.G.B.

* Corresponding author [telephone (314) 362-3344; fax (314) 362-7183; e-mail frieden@biochem.wustl.edu].

‡ Present address: Department of Chemistry, Wichita State University, 1845 Fairmount, Wichita, KS 67260.

[1] Abbreviations: CD, circular dichroism; NMR nuclear magnetic resonance spectroscopy; IPTG, isopropyl-*β*-D-thiogalactopyranoside; MOPS, 3-[*N*-morpholino]propanesulfonic acid; MSP, major spern protein.

10.1021/bi048614u CCC: $27.50
Published on Web 10/07/2004

Here, we again examined the folding of PapD, using ^{19}F NMR combined with fluorescence and CD, but monitoring the phenylalanine residues of PapD that have been labeled with *p*-^{19}F-phenylalanine. PapD contains six phenylalanine residues that are well dispersed throughout the sequence and are located in different environments (Figure 1). Phe 11, 86, 88, and 114 are positioned to report on the folding of the N-terminal domain. Phe 11, 86, and 88 are buried within the core of the N-terminal domain, whereas Phe 114 is located at the domain−domain interface. Phe 114 may, along with the potential to monitor the formation of the domain−domain interface, also provide information on the formation of complexes with pilus subunits (*4*). Phe 168 and Phe 205 are located in the C-terminal domain, are also buried residues, and are distant from the one tryptophan residue (Trp 128) and the domain−domain interface. Phe 205 is near the single disulfide bond in PapD formed by Cys 207 and Cys 212 and may provide information on the time frame that this region forms.

The structure of PapD with the phenylalanine and tryptophan residues identified is shown in Figure 1. As was reported previously for the C-terminal domain resonance of 6-^{19}F-Trp 128, new resonances are observed for *p*-^{19}F-Phe 168 and 205 that remain visible at denaturant concentrations beyond the loss of native resonance intensity. These same resonances are also observed to form rapidly upon refolding from the equilibrium denatured state. Furthermore, we find that *native* intensity for Phe 168 and Phe 205 is also observed to form early along with the intermediate, preceding the formation of observable native intensities for the N-terminal domain residues. Although no intermediate resonances are apparent for the N-terminal domain, there is significant missing intensity for this domain that may indicate some early structure formation (*5*).

The formation of the native N-terminal domain resonances, the loss of the intermediate resonances, and the continued formation of the native C-terminal domain resonances occur concomitantly and are slow processes, consistent with previous studies (*3*). To determine if this is because of a slow trans−cis isomerization event in the N-terminal domain itself, we performed ^{19}F NMR double-jump experiments to monitor the effect of proline isomerization on folding (*6*). The double-jump data indicate that the rate-limiting step in the folding of PapD is the slow folding of the N-terminal domain itself and specifically the trans−cis isomerization of one or both of the two cis prolines. The data indicate that the formation of native structure in the N- and C-terminal domains is a prerequisite for the formation of domain−domain interactions.

MATERIALS AND METHODS

Chemicals. All of the amino acids and reagents used for the preparation of the minimal media were from Sigma (St. Louis, MO). Ultrapure urea was obtained from United States Biochemical. Reagents for the preparation of Luria Bertani (LB) medium were from Difco. Enzymes used in the subcloning procedures were from New England Biolabs. For the PCR of the *papD* gene from pLS101 (*7*), we used the Proofstart PCR kit from Qiagen.

Strains and Vectors. The strain used for complete labeling (NK6024; CGSC#6178) and the strain for site-specific labeling (K10F6Δ) have been described (*8*). The latter was obtained as a generous gift from Dr. David Tirrell (California Institute of Technology, Pasadena, CA). Standard PCR strategies were used for subcloning the gene encoding PapD in pLS101 (*7*) into the Qiagen vector pQE80L (pQE80PapD) and include the signal sequence required for export to the periplasm. Mutagenesis of the Phe codons in pQE80PapD to amber codons was done using the QuikChange mutagenesis kit (Stratagene, La Jolla, CA). The resulting plasmids were used for complete labeling of the phenylalanine residues in NK6024 (pQE80PapD) and also for site-specific labeling (pQE80PapD-amber mutants) after insertion of the PheRS gene. The PheRS expression cassette was obtained as a *Pvu*II restriction fragment from the plasmid pRO148 (*8*). This was then inserted into the *Sma*I site of the pQE80PapD-amber mutants. The plasmid pRO117, which encodes the yeast tRNA$^{Phe/amber-ext}$ expression cassette, has also been described (*8*).

Complete and Site-Specific Labeling. For complete labeling, NK6024/pQE80PapD was grown in 5 mL of LB medium. From this, 1 mL was removed and diluted 1:1000 into 1 L of a minimal medium (*9*) containing 0.8 mM Phe and grown in a Fernbach flask overnight. This was then added to 12 L of the same minimal medium in a Bioflo 5000 fermentor (New Brunswick Scientific, Edison, NJ). A pH of 7.0 was maintained with 8.0 M ammonium hydroxide, the dissolved oxygen was maintained at or above 25%, and the glucose was maintained at 0.5%, which was monitored with urinalysis strips (*5*). Bacteria were grown to an OD_{600} of 3.0 and harvested in 1 L bottles. The cells were then washed twice with 0.9% NaCl and 1 mM *p*-^{19}F-Phe and then grown for 20 min in minimal medium supplemented with 1 mM *p*-^{19}F-Phe. IPTG was added to a final concentration of 1.0 mM, and the bacteria were allowed to grow for an additional 1 h (final $OD_{600} \sim 6.0$).

For site-specific labeling, 1 mL of cells (K10F6Δ/pQE80PapDPheRS/pRO117) was diluted from 5 mL of LB 1:1000 into 1 L of the same minimal medium only containing 0.2 mM Phe and 3.0 mM *p*-^{19}F-Phe. The cells were grown to an OD_{600} of 1.0, washed twice with 0.9% NaCl and 3 mM *p*-^{19}F-Phe, and then resuspended in 0.04 mM Phe and 3 mM *p*-^{19}F-Phe (*8*). After 20 min of growth, the cells were induced with 1.0 mM IPTG and grown for an additional 45 min−1 h. PapD was isolated from the periplasm as described previously (*1*). PapD was dialyzed against 20 mM MES/KOH, pH 6.0, and purified using Pharmacia SP Sepharose and Source 15Phe hydrophobic interaction chromatographies (Amersham Pharmacia, Piscataway, NJ). The concentrations of the purified protein were determined using an extinction coefficient of 24 977 M^{-1} cm^{-1}, as described previously (*3*).

Buffer. The buffer used in all experiments presented here is 30 mM MOPS/HCl, pH 7.0. For the NMR experiments, we include 30 μM 6-^{19}F-Trp as a standard and 10% D_2O.

Fluorescence. Emission spectra were recorded on an Alpha Scan PTI spectofluorometer (Photon Technologies, Ontario, Canada) using an excitation wavelength of 295 nm. The concentration for all fluorescence experiments was 1 μM. Stopped-flow experiments were performed using an Applied Photophysics SX.18MV (Applied Photophysics, Surrey, U.K.). Excitation was at 295 nm, the slits on the monochro-

mator were 2 mm, and the fluorescence above 320 nm was recorded using a cutoff filter.

Circular Dichroism. CD spectra were recorded using a Jasco J-715 spectropolarimeter. Equilibrium measurements were performed at a concentration of 21 μM, in a 0.1 cm path length cell. The response time was 2 s, and the scan rate was 20 nm per minute.

Stopped-flow CD experiments were performed with an Applied Photophysics RX1000 accessory equipped with a 0.2 cm flow cell. Final concentrations were 20 μM. Because there was only a small CD difference at 216 nm between folded and unfolded protein, measurements were recorded at 230 nm. In the presence of 6 M urea, however, the CD spectrum was that of an unfolded protein (data not shown). For data collected to 150 s, a response time of 0.125 s was used. For data to 5000 s, a response time of 2 s was used.

^{19}F NMR Spectroscopy. Fluorine NMR spectra were recorded on a Varian Unity-Plus 500 MHz spectrometer operating at 470.3 MHz with a Varian Cryo-Q dedicated 5 mm fluorine cryoprobe. The cryoprobe was maintained at 20 K with the Varian Cryo-Q Open Cycle cryogenic system. The t_1 relaxation times of the fluorine resonances were measured using the inversion recovery method as described previously (*3*). Sample concentrations were 70 μM for the experiments shown. Stopped-flow experiments were performed using an Applied Photophysics RX1000 mixer adapted for use as described elsewhere (*10*, *11*). Approximately 1 mL of freshly mixed solution displaces 90% of the old solution. The dead time of the mixer is estimated at 100 ms. Experiments were performed using a modified s2pul pulse sequence that delays acquisition until the user triggers the acquisition of data using the stopped-flow device. After an initial delay of 1.5 s to allow for magnetic equilibrium to be attained, data were recorded 1.24 s apart for 150 s. The data represent 48 separate injections, and the individual shots were summed as described previously (*3*). For the long time course experiment, data were recorded using the pad command in VNMR, such that each spectrum at a given time point represents 32 transients. Three separate injections from the long time course experiment were then summed to give the final time course of refolding as described previously (*3*).

^{19}F NMR Double-Jump Experiments. The double-jump experiments were performed as follows: The protein and urea were kept on ice. The protein was diluted to a final concentration of 7.5 M urea, being sure not to disturb the solution prior to mixing, which may cause crystallization of the urea. After the initial 110 s to allow unfolding, this mixture was then diluted on ice to 2.14 M urea, quickly placed in a prechilled NMR tube, and injected into the magnet with VT set to 5 ± 1.0 °C. Different periods of time after the 110 s unfolding were used before refolding. A single, 64-transient spectrum was then recorded.

Data Analysis. The fluorescence, CD, and ^{19}F NMR equilibrium unfolding transitions were fit to the two-state equation of Santoro and Bolen (*12*) using Kaleidagraph (Synery Software, Reading, PA). The amplitudes from the ^{19}F NMR data were obtained from fitting the individual fids using the Bayesanalyze program within VNMR (L. Bretthorst, Washington University) (*3*).

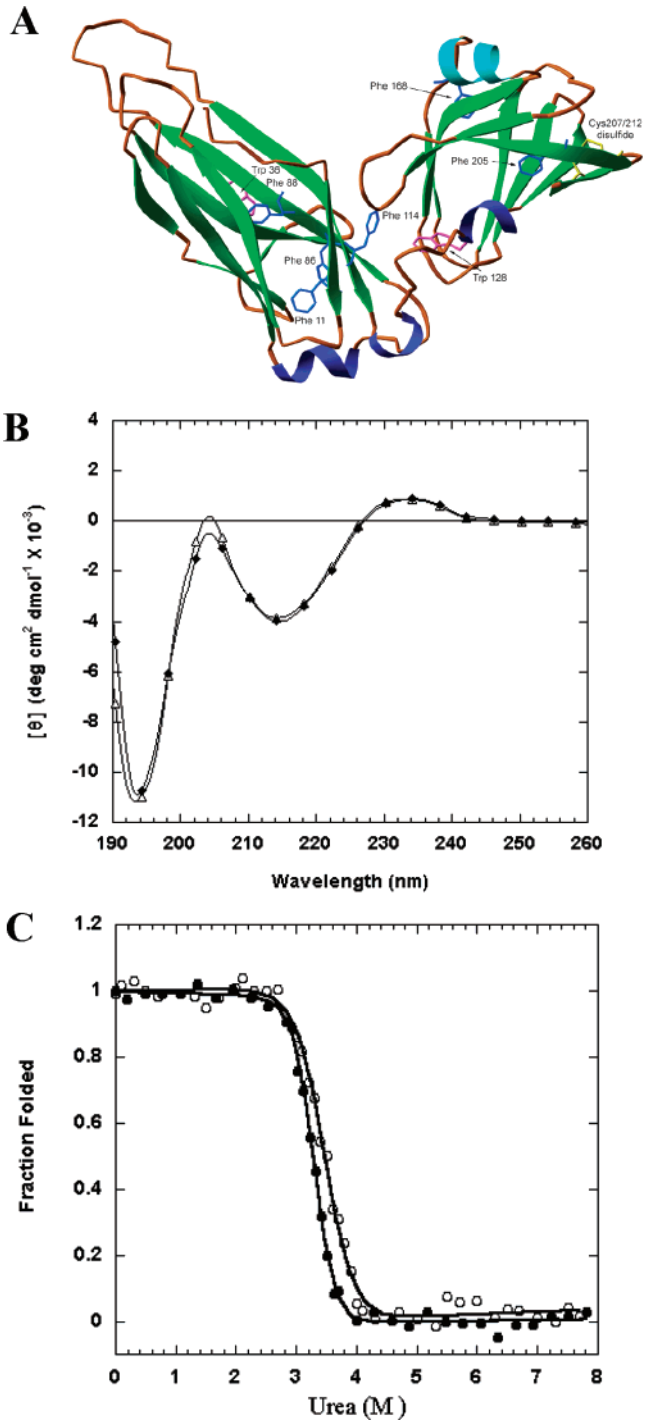

FIGURE 1: (A) Ribbon diagram of PapD (1PDK:A). The phenylalanine (Phe) residues are blue, and the tryptophan (Trp) residues are purple. The disulfide bridge at the end of the C-terminal domain is yellow. (B) CD spectra of PapD unlabeled (△) and *p*-^{19}F-Phe labeled (◆) at a concentration of 21 μM in 30 mM MOPS/HCl, pH 7.0. (C) Normalized fluorescence of PapD unlabeled (●) and *p*-^{19}F-Phe labeled (○) as a function of urea at 20 °C (ex, 295; em, 335 nm) in 30 mM MOPS/HCl, pH 7.0. Fluorescence was normalized using the equation $F_{norm} = F_{obs} - F_u/F_n - F_d$; F_n = native fluorescence, F_d = denatured fluorescence. The fluorescence data shown are corrected such that the slopes of the folded and unfolded states are zero.

RESULTS

^{19}F NMR: Assignment of the ^{19}F-Phe Resonances. In 1998, Fürter described a novel method for the insertion of a single ^{19}F-Phe amino acid into mouse dihydrofolate reductase (*8*).

Table 1: Thermodynamic Parameters for Unfolding of *p*-^{19}F-Phe-Labeled PapD

method	ΔG^a (kcal/mol)	m^a (kcal/mol/M)	$\Delta G/m$ (M)
fluorescence wild type[b]	8.95 ± 0.4	2.7	3.31
fluorescence *p*-^{19}F-Phe-labeled	6.2 ± 0.4	1.8	3.44
^{19}F NMR Phe 11 N[c]	7 ± 2	2	3.5
^{19}F NMR Phe 86 N	8.2 ± 3.6	2.4	3.4
^{19}F NMR Phe 88		ND[c]	
^{19}F NMR Phe 114 N	7 ± 6	2	3.5
^{19}F NMR Phe 11, 86, 114 D[c]	7.45 ± 1	2	3.7
^{19}F NMR Phe 168 N	6.8 ± 3.4	1.9	3.57
^{19}F NMR Phe 168 D	8.4 ± 0.5	1.9	4.4
^{19}F NMR Phe 205 N	7.3 ± 2.6	2.1	3.48
^{19}F NMR Phe 205 D	10.5 ± 0.8	2.3	4.56

[a] Obtained from a nonlinear least-squares fit according to the method of Santoro and Bolen (*12*). [b] Fluorescence data are taken from ref *3*. [c] Phe 88 native (N) and denatured (D) resonances overlapped, and the denatured resonances of Phe 11, 86, and 114 also overlapped and could not be resolved. The fit represents the sum amplitude of these resonances shown in Figure 2B.

This method utilizes a heterologous yeast amber tRNA^{Phe}/PheRS system in *Escherichia coli* to incorporate *p*-^{19}F-Phe at AUG amber stop codons in the sequence of the protein to be labeled. We have shown previously that the method can be successfully applied to assign the native ^{19}F-Phe resonances of PapD (*13*). The chemical shifts for the individually labeled proteins did not differ significantly from that of the fully labeled protein, indicating that there is little effect on the structure of the protein (*13*).

Urea-Induced Unfolding Transitions of Unlabeled and p-^{19}F-Phe-Labeled Proteins. The CD spectra of the unlabeled and *p*-^{19}F-Phe-labeled proteins are shown in Figure 1B. The differences in stability between the unlabeled and labeled proteins were determined by equilibrium denaturation experiments using fluorescence (Figure 1C), and the data are summarized in Table 1. Previous experiments have shown that PapD undergoes a cooperative two-state transition when measured by fluorescence or CD changes at 230 nm, with both methods providing nearly identical results. For the *p*-^{19}F-Phe-labeled protein, the spectral changes as a function of urea closely match that of the unlabeled protein, indicating that fluorine labeling has not greatly affected the stability of the protein. Also, the secondary structure as measured by CD has not been affected, indicating that fluorine labeling has not changed the structure of the protein.

Urea-Induced Unfolding As Monitored by ^{19}F NMR: Equilibrium Experiments. Figure 2A shows the ^{19}F NMR spectra of fully labeled PapD as a function of urea concentration. Several points are immediately apparent. First, we note that the two native resonances of Phe 11 and Phe 168 shift well before the appearance of denatured resonances and that the shifts are in opposite directions, whereas other resonances appear to shift very little. Phe 11 and 168 are predicted to be inaccessible to solvent (*14*), but there may be effects from urea on the local structure surrounding these residues that are reflected in these chemical shift changes. There are no significant chemical shift changes for the native resonance of Phe 114 that lies between the two domains. This resonance is, however, broader than the other resonances and may be indicative of a relaxation mechanism that involves interdomain motions (see Figure 1A). Second, the two native resonances of Phe 168 and 205 split to separate resonances (F168 I and F205 I) as the concentration of urea increases, and these new resonances persist at urea levels at which the native N- and C-terminal domain resonances have disappeared. Finally, four peaks are observed in the denatured protein, three of which are identifiable as specific residues (F88, F168, and F205 D).

The amplitudes of the resonances as a function of urea for the N- and C-terminal domains are also shown in Figure 2B. The loss of the native N- and C-terminal domain intensities occurs at similar denaturant concentrations, indicating a concomitant loss of native structure for the two domains (*3*). Also, the loss of native intensity mirrors the changes observed by fluorescence and CD, indicating that these techniques are monitoring the same loss of native structure. In contrast to our previous study, the amplitudes of the intermediate species are much greater, and at 4 M urea are >50% of the initial native amplitudes. The intermediate intensities of Phe 168 and 205 persist at higher denaturant concentrations than was observed previously with 6-^{19}F-Trp 128 and are reflected in the higher midpoint for the unfolded resonances of the C-terminal domain. This suggests that the intermediate is more highly populated than previously observed.

Although we observed a concomitant loss of native intensity for the N- and C-terminal domain resonances, the persistence of intermediate resonance intensity for Phe 168 and 205 suggested that perhaps fluorine labeling one or both

Table 2: Kinetic Data for *p*-^{19}F-Phe-Labeled PapD Refolding[a]

method	A_1	k_1 (s^{-1})	A_2	k_2 (s^{-1})	A_3	k_3 (s^{-1})
fluorescence (WT)	0.21 ± 0.001	2.5 ± 0.03	0.06 ± 0.0007	0.07 ± 0.003		
fluorescence (*p*-^{19}F-Phe)	0.25 ± 0.001	3.35 ± 0.03	0.04 ± 0.001	0.077 ± 0.006	0.6	0.00067
CD *p*-^{19}F-Phe	0.4 ± 0.02	1.7 ± 0.2	0.2 ± 0.02	0.05 ± 0.02	0.6	0.00048
^{19}F-Phe 11 N					529[b]	0.00068
^{19}F-Phe 86 N					524	0.00086
^{19}F-Phe 88					850	ND
^{19}F-Phe 114 N					717	0.00088
^{19}F-Phe 11, 86, 114 D			500[b]	0.029	1268	0.00086
^{19}F-Phe 168 N				0.03	340	0.002
^{19}F-Phe 168 I			490	ND	366	0.00088
^{19}F-Phe 205 N				0.024	395	0.00086
^{19}F-Phe 205 I			492	ND	311	0.0009

[a] Refolding was carried out in 30 mM MOPS/HCl, pH 7.0, at 20 °C, 2.14 M urea final concentration. The final concentration for the fluorescence data was 1 μM. The CD and ^{19}F NMR data were recorded at a final concentration of 20 μM. Stopped-flow NMR data were recorded in 30 mM MOPS/HCl, pH 7.0, 10% D_2O, 0.3 mM 6-^{19}F-Trp (as a standard). [b] The ^{19}F NMR relative amplitudes and rate constants were obtained from Bayesian analysis. ND indicates that the changes were too fast to be determined by ^{19}F NMR.

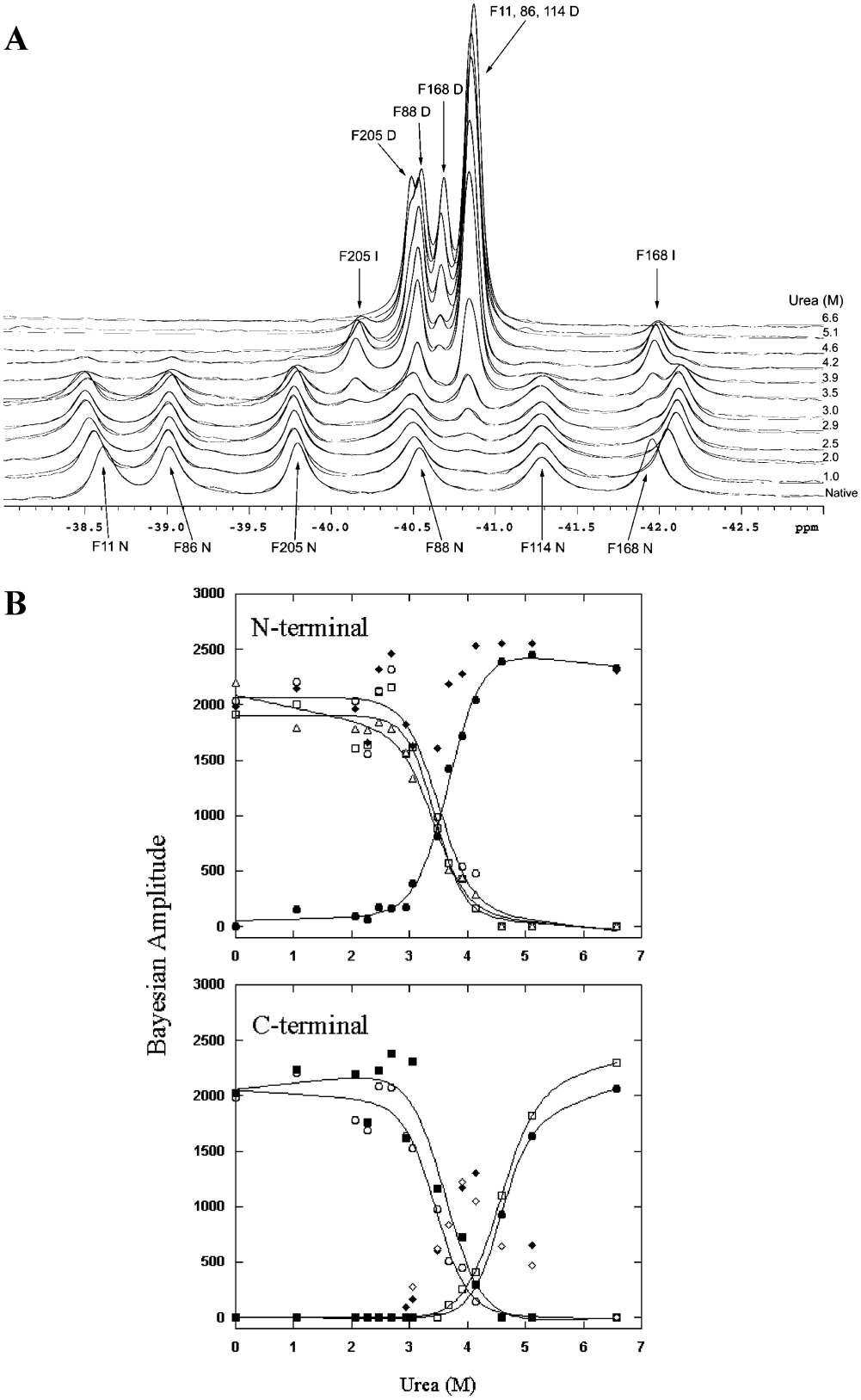

FIGURE 2: (A) ^{19}F NMR spectra of *p*-^{19}F-Phe-labeled PapD as a function of urea at 20 °C. The concentration of PapD was 70 μM in 30 mM MOPS/HCl, pH 7.0, 10% D_2O, and spectra were referenced to an internal standard of 6-F-Trp (0.3 mM). N, I, and D represent native, intermediate, and denatured resonances, respectively. The lines through the spectra are best fits using Bayesian analysis. (B) Amplitudes of the ^{19}F NMR data in (A) as a function of urea: (top) N-terminal domain resonances of Phe 11 native (△), Phe 86 native (□), Phe 88 native/denatured (◆), Phe 114 native (○), and the sum of the denatured resonances of Phe 11, 86, and 114 (●); (bottom) C-terminal domain resonances of Phe 168 native, intermediate, and denatured (■, ◆, □) and Phe 205 native, intermediate, and denatured (●, ◇, ○).

of these residues selectively stabilized the C-terminal domain. The insertion of a fluorine atom into a protein has been shown to have either stabilizing or destabilizing effects on stability (*13*, *15*−*17*). To determine if there was a selective stabilization of this domain by fluorine, we site-specifically labeled Phe 168 and Phe 205 individually with *p*-^{19}F-Phe

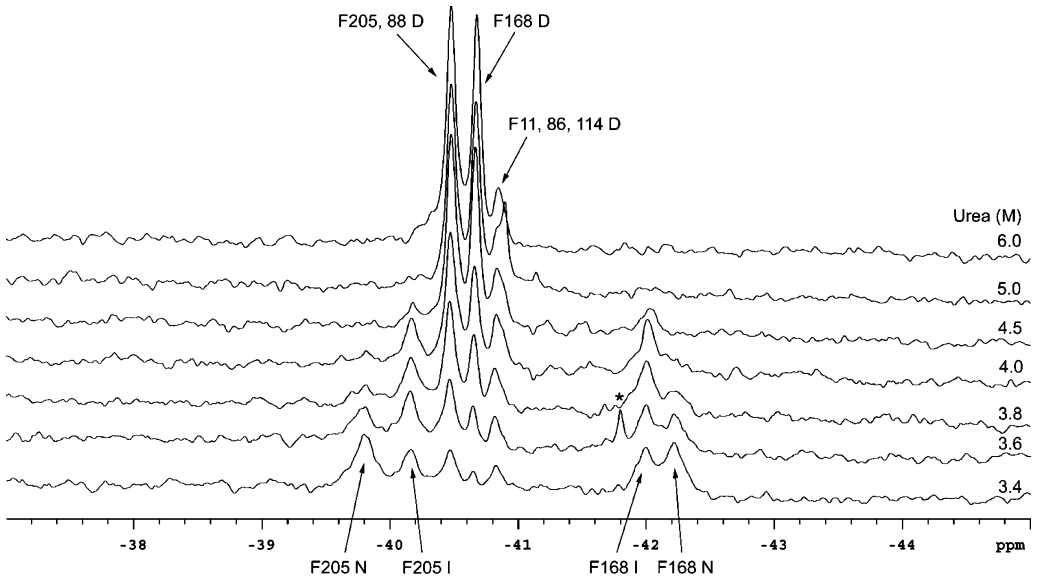

FIGURE 3: ^{19}F NMR spectra of *p*-^{19}F-Phe-labeled PapD Phe 168-amber and Phe 205-amber as a function of urea at 20 °C. N, I, and D represent native, intermediate, and denatured resonances, respectively. The separately purified proteins were combined such that the amplitudes of the native resonances were similar (~3-fold higher concentration of Phe 205 relative to Phe 168). The final concentration of Phe 168 was 70 μM, and data were recorded in 30 mM MOPS/HCl, pH 7.0, 10% D_2O, and 6-F-Trp (0.3 mM). The asterisk (*) indicates a likely impurity.

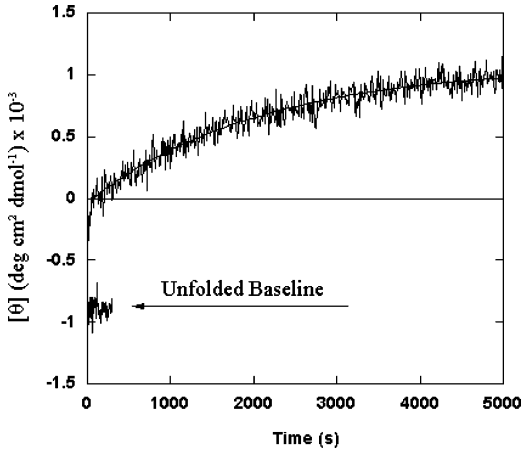

FIGURE 4: Stopped-flow CD data of *p*-^{19}F-Phe-labeled PapD at 20 μM for a urea jump from 7.5 to 2.14 M. The unfolded baseline (7.5 M urea) is shown along with the time course of refolding of PapD. The refolding conditions were 30 mM MOPS/HCl, pH 7.0, 20 °C.

and measured the stability to denaturant by ^{19}F NMR (Figure 3). To match the urea concentration, both proteins were combined such that the native ^{19}F NMR resonances matched intensity (requiring ~3-fold more Phe 205-amber than the Phe 168-amber mutant) and added to NMR tubes containing urea to give the final urea concentration shown. Although the signal-to-noise is somewhat poor, the data indicate that the disappearance of native and intermediate resonances occurs at the same denaturant concentration, and therefore the persistence of intermediate intensity is likely not a consequence of the fluorine labeling at these positions.

Kinetics of Folding of PapD Measured by Fluorescence and Circular Dichroism. Figure 4 shows the stopped-flow data for refolding from 7.5 M urea to 2.14 M at 20 °C and pH 7.0 monitored by CD at 230 nm. In previous experiments we used a urea jump from 4.5 to 2.25 M urea, because by ^{19}F NMR, fluorescence, and CD the protein was >95% unfolded at 4.5 M urea (*3*). Because of the persistence of the *p*-^{19}F-Phe intermediates at 4.5 M urea, we chose to initiate refolding from 7.5 M urea, at which we had no evidence of residual structure. The kinetic data indicate the presence of three separate phases, which are summarized in Table 2. Also summarized are stopped-flow fluorescence data obtained at a concentration of 1 μM. The rate constants of these phases using either technique are similar, indicating that both are likely to be reporting on the same events during folding. A rapid change in CD at 230 nm precedes the slow phase, and we attribute this rapid change to the collapse of the C-terminal domain (*3*).

Kinetics of Folding of PapD As Measured by Stopped-Flow ^{19}F NMR. Figures 5 and 6 show the time course of folding of the individual residues as measured by stopped-flow ^{19}F NMR using a urea jump from 7.5 M to a final concentration of 2.14 M. The data are also summarized in Table 2. The stopped-flow data indicate that there is a rapid formation of structure around Phe 168 and Phe 205, indicating that the C-terminal domain collapses early (see inset at 2.74 s in Figure 5). In contrast to our previous study, native intensity is also apparent along with intermediate intensity. The native resonances of the C-terminal domain continue to form as the intermediate resonances disappear. The rate of formation of the Phe 168 native intensity is ~2-fold faster than the appearance of the Phe 205 native intensity and is observed at either a different urea jump (from 4.5 to 2.25 M) or if the final concentration of protein is halved (35 μM). However, the rate of loss of intermediate intensity is the same as the appearance of native Phe 205 intensity (Figure 6). The native resonances in the N-terminal domain appear at the same slow rate as the loss of denatured resonance intensity, and at the same rate as the (continued) formation of native Phe 205 intensity. At the beginning of folding, we note that there is a substantial amount of intensity missing from the N-terminal domain denatured resonances of Phe 11, 86, 88, and 114 (Figure 5, peak 3). Figure 7 shows the summation of resonance intensity for the N- and C-terminal domain resonances as a function of time at 70

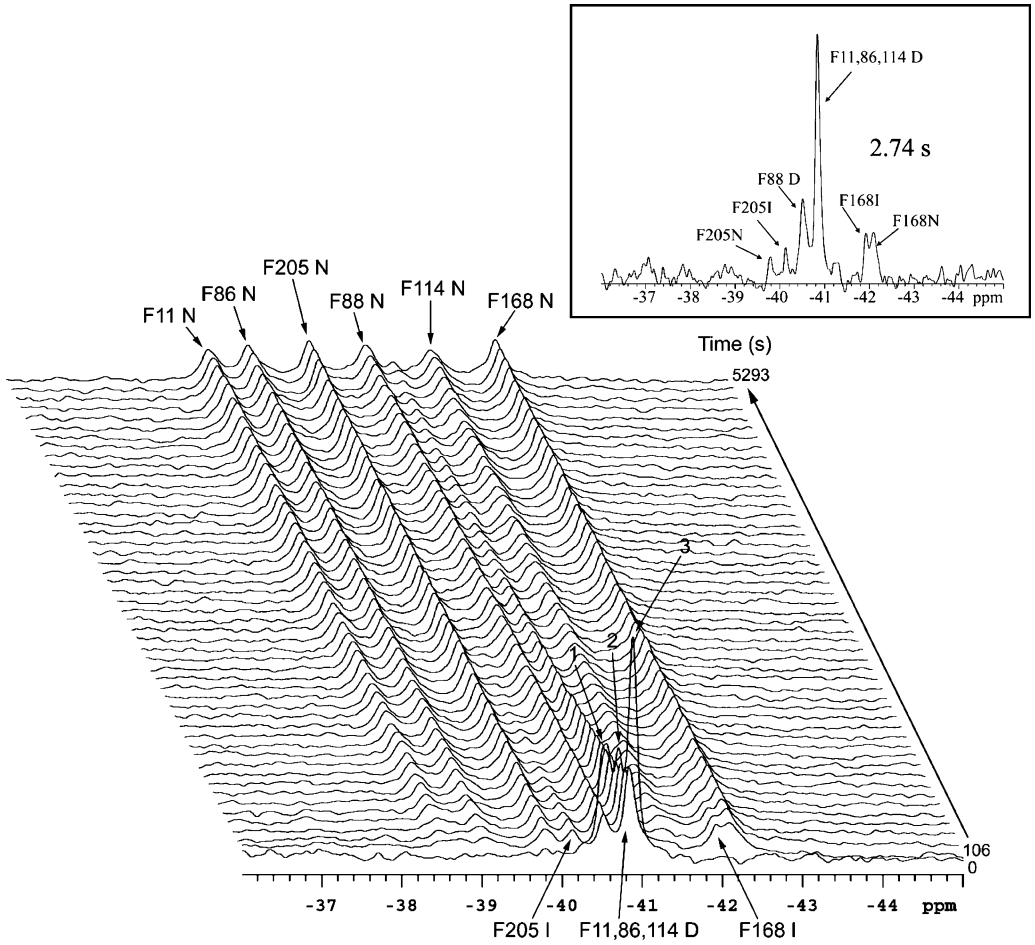

FIGURE 5: ^{19}F NMR stopped-flow refolding kinetics of *p*-^{19}F-Phe-labeled PapD. The final concentration was 70 μM, and spectra were recorded at 20 °C in 30 mM MOPS/HCl, pH 7.0, 10% D_2O, and an internal standard of 6-^{19}F-Trp (30 μM). Refolding was initiated by a rapid jump from 7.5 to 2.14 M urea using a stopped-flow apparatus mounted on the magnet (see Materials and Methods). (Inset) Initial timepoint at 2.74 s after mixing. The 90° pulse was 6.3 μs, and the pulse sequence included a 3.1 s delay and an acquisition time of 200 ms. Spectra were arrayed using the pad command in VNMR, and 32 transients were collected between each pad (no delay). Each spectrum represents the sum of three separate injections. 1, 2, and 3 correspond to the denatured resonances of Phe 88 and 205, the denatured form of Phe 168, and the denatured form of Phe 11, 86, and 114, respectively.

and 35 μM final concentrations. Comparison of the zero time point (denatured) and the earliest refolding time point indicates that there is missing intensity for the N-terminal domain resonance but not for the C-terminal domain resonances and that there is clear missing intensity that rises at the same rate as the stabilization of the other resonances. Because the amplitudes for the C-terminal domain resonances are unchanged throughout the time course, this indicates that this unaccounted for missing intensity is likely not due to aggregation. Furthermore, the same loss of intensity is observed at half the protein concentration (35 μM), and the rate constants for the faster phases obtained by stopped-flow CD at 20 μM are similar to that observed by fluorescence (1 μM final). Finally, a shallower urea jump to a similar final denaturant concentration (4.5 M to 2.25) has little effect on the disappearance of intensity.

Double-Jump ^{19}F NMR Experiments. To determine if the observed slow folding of PapD was because of the trans to cis isomerization of proline of either Pro 49 or Pro 54 (which are cis in the native state) in the N-terminal domain, we performed double-jump experiments using ^{19}F NMR (Figure 8A). Because of the need to use urea as a denaturant, we performed the double-jump experiments at low temperature (5 °C) to prevent significant isomerization from occurring prior to unfolding. The rate of unfolding in urea as measured by fluorescence (1 μM) was independent of temperature from 20 to 5 °C, with a rate constant of ~0.14 s^{-1}, and at 5 °C is expected to be faster than proline isomerization (data not shown). At different times after unfolding in 7.5 M urea, the protein was diluted to 2.14 M urea, and the NMR spectra were recorded with time. At the shortest time allowable for recording a spectrum (~110 s for denaturation and then a jump back to 2.14 M urea), the spectra show that all of the native intensity is present, with only some intensity apparent for the denatured form of Phe 11, 86, 88, and 114. With increased time of denaturation, the native resonances of the N-terminal domain decrease, whereas the N-terminal domain denatured resonances accumulate. However, while the native resonances of Phe 168 and Phe 205 decrease, the intermediate resonances accumulate. Importantly, the rate constant for the disappearance of the native resonances of Phe 11 and 86 in the N-terminal domain corresponds to the rate of cis to trans isomerization at this temperature (Figure 8B) (*18*). This indicates that one of the cis proline residues, either Pro 49 or Pro 54, is required to isomerize back to the cis conformation to form the native state of the N-terminal domain and allow the subsequent formation of domain−domain interactions.

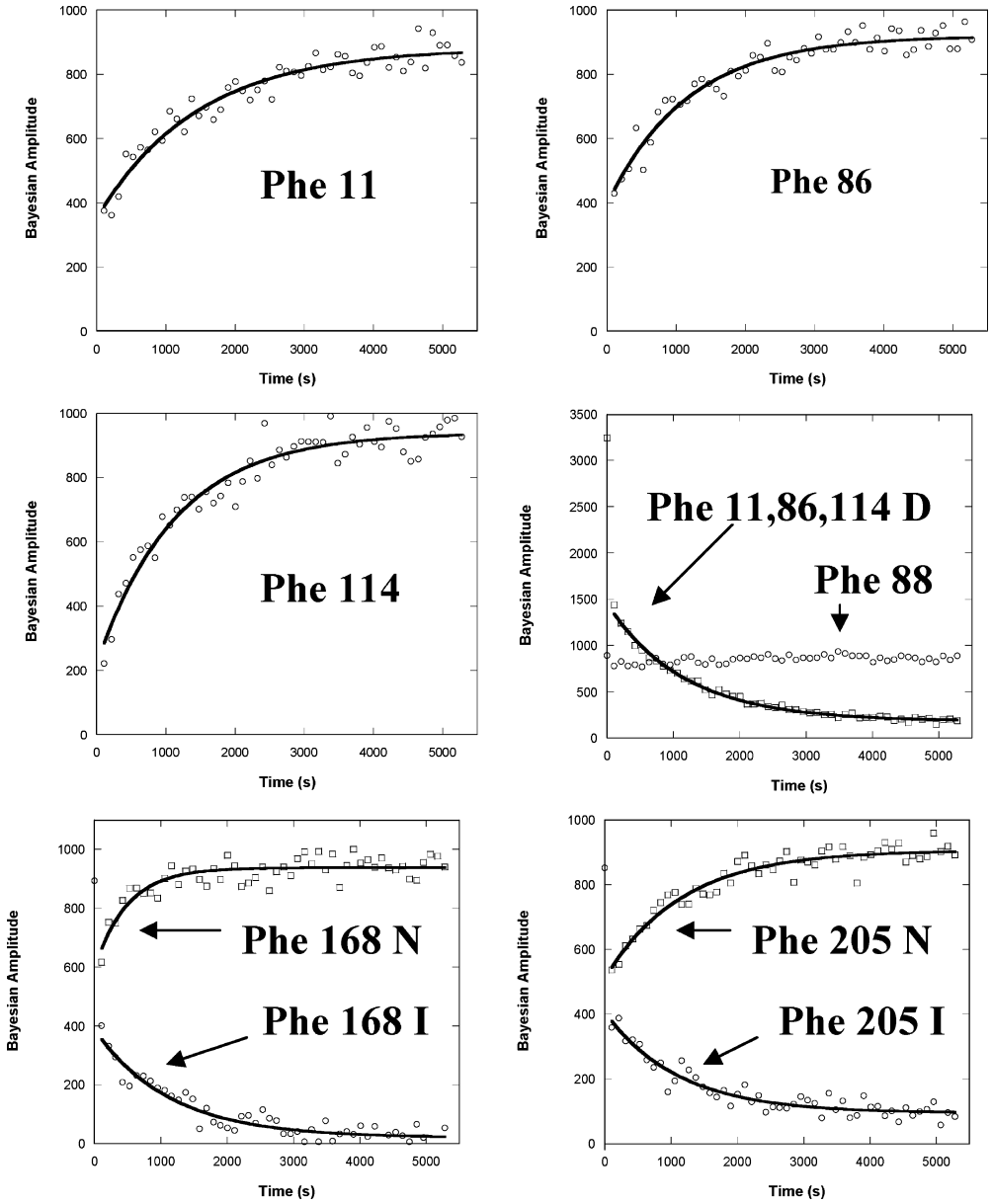

FIGURE 6: Analysis of ^{19}F NMR stopped-flow kinetics data: (○) native resonances for the N-terminal domain and for the intermediate resonances of Phe 168 and 205; (□) native resonances for Phe 168 and 205 and for the denatured resonance of Phe 11, 86, and 114. The amplitudes were obtained from the data in Figure 5 using Bayesian analysis. The solid line through the curves represents the best fit to a single-exponential rate function.

DISCUSSION

The experiments described here using *p*-^{19}F-Phe-labeled PapD indicate that the folding process from an equilibrium denatured state involves three sequential events: (1) the initial collapse of the C-terminal domain, (2) the trans to cis isomerization of proline in the N-terminal domain, and (3) the formation of domain−domain interactions. From the ^{19}F NMR kinetics folding data, intermediate and native side-chain intensities for the C-terminal domain are observed early on and with nearly equal intensity. This indicates that the rate of stabilization of the Phe 168 and Phe 205 side chains was faster than what we had observed previously for Trp 128, where no native resonance intensity was observed at the earliest time point (*3*). One reason for this difference may be due in part to the proximity of these side chains to the domain−domain interface. Trp 128 is close to the domain−domain interface, and the rate of formation of native intensity was concomitant with the rate of stabilization of Trp 36 in the N-terminal domain and, thus, the entire protein (*3*). Phe 168 and 205 are more distant from the domain−domain interface, and the side chains project into the core of the C-terminal domain. Phe 168 is in the D strand of the C-terminal domain and is near the α-helix between the C and D strands. The rate of formation of this helix may be the initial site of nucleation for the C-terminal domain and may affect the rate of formation of Phe 168, which was observed to be ∼2-fold faster than the rate of stabilization of Phe 205. Phe 205 is only two residues away from the disulfide bond formed between Cys 207 and Cys 212 but, interestingly, showed a rate of stabilization similar to that of the N-terminal domain resonances. These data suggest that side chains stabilize (even within the same domain) at different rates during the folding process, a point that has been largely overlooked (*19*).

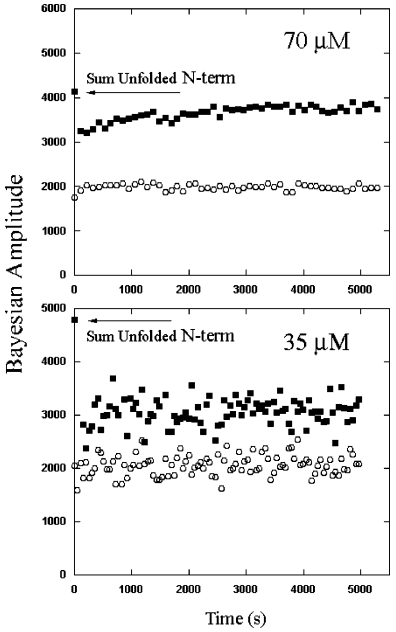

FIGURE 7: Plots of total resonance intensity from ^{19}F NMR stopped-flow kinetics data. The data are separated into resonances from the N- and C-terminal domains at final concentrations of 70 μM (top) and 35 μM (bottom). Note the initial loss of amplitude from the sum of unfolded resonances for the N-terminal domain to the initial time point obtained using the stopped-flow apparatus.

The intermediate resonances that appear early in the kinetics studies also appear in the equilibrium denaturation experiments. This is consistent with our previous study in which an intermediate is observed from the C-terminal domain residue Trp 128 that persists beyond the loss of native resonance intensity and is reversible (*3*). However, in the previous study intermediate intensity is observed until ~4.5 M urea, whereas the intermediates of Phe 168 and Phe 205 persist at >5 M urea. Furthermore, whereas for the 6-^{19}F-Trp-labeled protein the maximum population of intermediate intensity approached only 10% of the native intensity, the maximum intermediate intensity for the *p*-^{19}F-Phe-labeled protein is >50% of the native intensity (Figure 2). Therefore, Phe 205 and Phe 168 may be in more stable environments in the intermediate state, which may be a reflection of the faster rate of stabilization. In separate ^{19}F NMR kinetics measurements, the rate of formation of the intermediates of Phe 168 and 205 from a urea jump of 8 to 4 M (where no native intensity is present) shows that the intermediates can form within 10 s, with no evidence of native intensity (data not shown). Again, this suggests that the intermediates observed are stable and can form reversibly, indicating that they are on-pathway.

The persistence of intermediate resonance intensity in equilibrium experiments suggests that the C-terminal domain can exist as a stable independently folding unit, whereas the N-terminal domain likely requires interactions from the C-terminal domain for stability. This difference in stability may be a consequence of the single disulfide bond present at the C terminus. Mutagenesis of both of the two cysteines Cys 207 and 212 to serine significantly destabilizes PapD and prevents the formation of pili (*20*) at 37 °C. Recent experiments also indicate that mutation of the two cysteines to alanines also destabilizes PapD and results in a very slow refolding process that requires days to reach equilibrium (J. Bann, unpublished observations). The disulfide is distant from the domain−domain interface, so maintaining the native structure of the C-terminal domain is important for the stability of the entire PapD structure. In other experiments, we have shown that the C-terminal domain (residues 119−214) can be stably produced in the periplasm at 37 °C, whereas expression of the N-terminal domain (residues 1−118) is not detectable in the periplasm at 20 or 37 °C (J. Bann, unpublished observations). This is despite both domains being expressed from identical plasmids and both encoding the native *papD* signal sequence. Similar findings have been reported by Hermanns et al. on the PapD homologue FimC (which does *not* have a disulfide), in that the C-terminal domain could be produced (in the cytoplasm) and under no conditions was a stable N-terminal domain observed (*21*).

The observation that the N-terminal domain cannot be expressed alone may not be so unusual. Proteins that exhibit structural homology to the N- and C-domains include, respectively, the major sperm protein (MSP) and the small α-amylase inhibitor Tendamistat (*22*−*25*). Whereas Tendamistat is monomeric in solution, the MSP is a homodimer (*26*). The homodimer interface of MSP is similar to the interface between the two domains of PapD (*22*), suggesting that the N-terminal domain structure may not exist in nature as a monomer and may require the C-terminal domain for stabilization.

Although there is no evidence during the initial stages of refolding that the N-terminal domain Phe side chains have stabilized, there is substantial missing intensity from the denatured side chains of Phe 11, 86, and 114 that may indicate the formation of a meta-stable structure (Figures 6 and 7). Previous kinetics studies of *E. coli* dihydrofolate reductase have also shown missing intensity early in the refolding process that was attributed to the presence of a dry molten globule (*5*). The dry molten globule was described as the formation of native-like secondary (as measured by CD) and tertiary structure where solvent has presumably been excluded from the core but where the side chains have not been stabilized (*5*). Previously we hypothesized that the slow formation of the positive CD at 230 nm was evidence of the formation of secondary structure in the N-terminal domain of PapD. Although the poly(L-proline) II helix contributes to this region (*27*), studies on the cardiotoxins and neurotoxins from snake venom have shown that the CD at 230 nm is likely a contribution from a tyrosine side chain rather than a regular secondary structure (*28*, *29*). Therefore, our data cannot discount the possibility that the N-terminal domain also forms a dry molten globule that includes the early formation of secondary structure that the CD at 230 nm is not sensitive to. However, this structure is likely to be in rapid exchange with other conformations that make its detection as a separate resonance difficult.

From the equilibrium denatured state, the trans to cis isomerization of one of the cis proline residues in the N-terminal domain must occur to form the native structure. In the unfolded state the trans form constitutes ~90% of the proline forms on the basis of the PapD sequence and the data of Reimer et al. (*18*). This in conjunction with the double-jump experiments indicates that proline isomerization is rate limiting in the slowest phase of refolding.

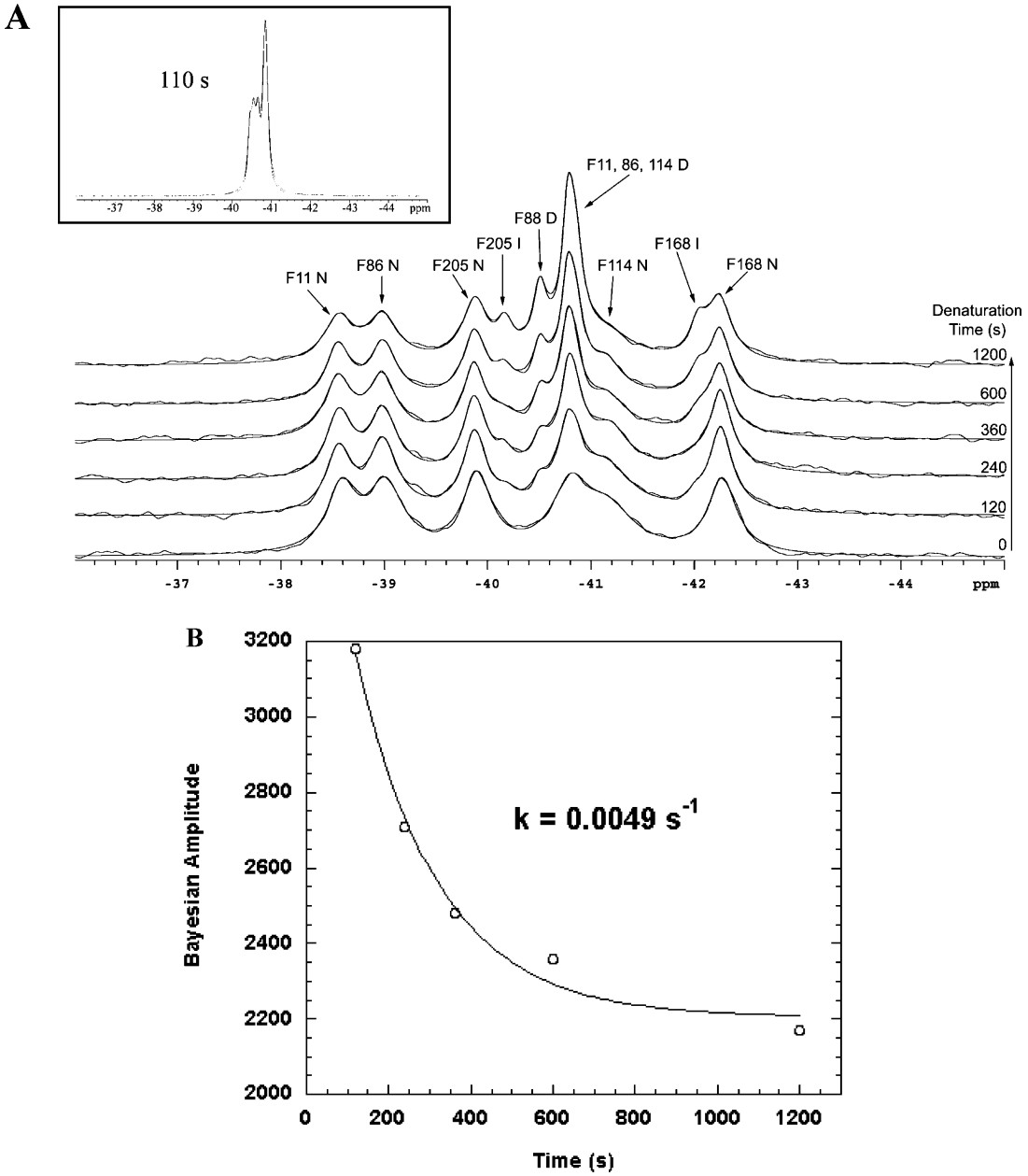

FIGURE 8: (A) ^{19}F NMR double-jump refolding of *p*-^{19}F-Phe-labeled PapD. The double-jump experiments were conducted at 5 °C. The samples and urea were kept on ice prior to insertion in the magnet. The samples were diluted into a tube containing urea and allowed to incubate for the specified time. After the initial denaturation period in 7.5 M urea, the samples were then diluted back to 2.14 M. The sample was then placed into a chilled NMR tube and quickly inserted into the magnet, which was at 5 ± 1 °C. The spectrum at 0 time was taken with a sample that had not undergone a double jump, but had simply been brought to 2.14 M urea on ice. (Inset) Spectrum after 110 s in 7.5 M urea. (B) Amplitude of Phe 86 as a function of time of denaturation. The solid line through the curve is a best fit to a single-exponential rate function.

Neither of the two cis proline residues is near the domain−domain interface, suggesting that the influence on domain−domain interactions is through a secondary effect on the structure of the N-terminal domain itself (Figure 9). Although we cannot rule out the role of Pro 49 (which is also cis in the native structure), Pro 54 is conserved among all chaperone sequences found to date as well as MSP (*22*). This cis proline induces a kink in the middle of the *D* (*D*′ and *D*″) strand that initially forms a hydrogen bond with the E strand and then switches to the C strand midway through the sequence (Figure 9). A hydrogen bond is formed from the carbonyl of the Thr 53−Pro 54 imide to the amide NH of Arg 68 (E strand). Mutation of Pro 54 to either Ala or Gly results in barely detectable levels of protein in the periplasm compared to wild-type or Pro 49 Ala/Gly mutants (data not shown). This indicates that the in vivo stability of PapD is compromised to a greater extent if the cis Pro 54 is absent and may be because of the inability to form either the hydrogen bond or the subsequent kink.

The equilibrium ^{19}F NMR data show that as the protein is unfolded, all of the native resonances disappear concomitantly, and the kinetics data show that the regaining of native intensity is also concomitant between the two domains. Although Phe 114 is ideally suited for monitoring the formation of domain−domain interactions, the rate of formation of this resonance matched the rate of appearance of Phe 11 and 86 (Figure 6 and Table 2). Because of

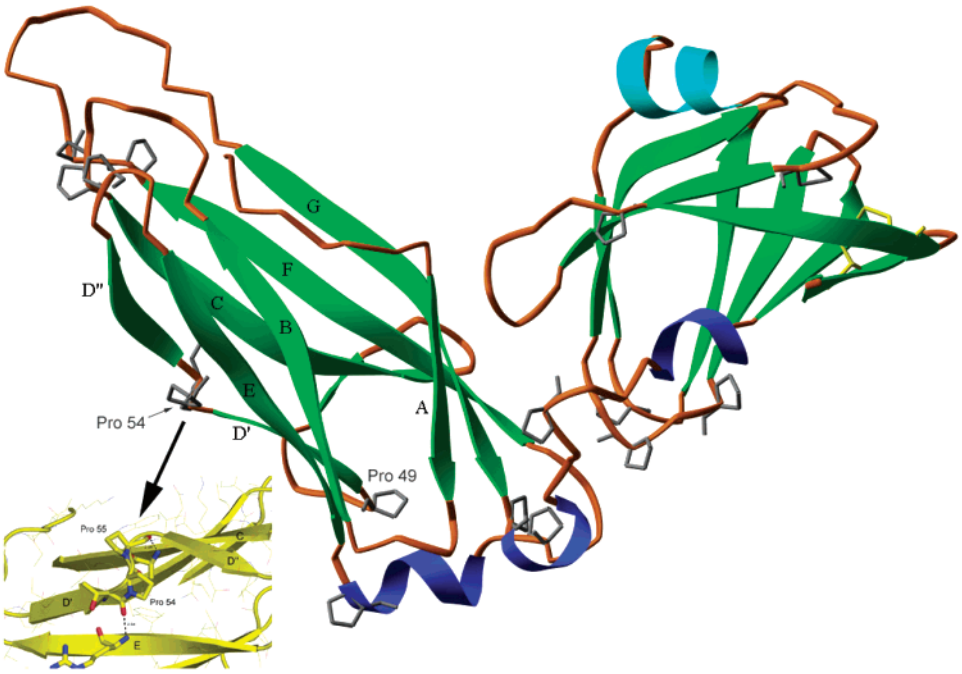

FIGURE 9: Ribbon diagram of PapD showing the proline residues. Both Pro 49 and Pro 54 are distant from the domain−domain interface. (Inset) Blowup of the region around Pro 54, showing the hydrogen bond of the carbonyl of Pro 54 to the amide hydrogen of Arg 143 in the E strand.

the slow rate-limiting proline isomerization process, we could not determine the rate at which the domains come together after this process has occurred. However, on the basis of the ^{19}F NMR double-jump experiments, when the N-terminal domain proline residues are in their native cis conformation (and thus a native N-terminal domain), the formation of domain−domain interactions is fast. Therefore, the formation of domain−domain interactions may be rapid enough to appear concomitantly with the formation of native structure in the N-terminal domain.

In conclusion, our data support the model put forth by Brandts and co-workers, where it is assumed that interactions between domains can exist only if both domains are in a native state (*30*). The unfolding of either domain causes the free energy of interaction between both domains (ΔG_{AB}) to go to zero, such that the loss of native structure should be a concomitant process. Such is the case with PapD, using ^{19}F NMR, CD, or fluorescence. In multidomain proteins as well as non-covalent domain−domain complexes, the formation of the interface typically involves the burial of a considerable amount of surface area (*31*−*33*). There are extensive interactions at the interface between the two domains of PapD that involve both hydrophobic and salt bridge contacts. Two negatively charged residues, Glu 83 and Asp 196, form a highly conserved salt-bridge to Arg 116 that is proximal to the linker that connects the two domains (*4*, *34*, *35*). Mutagenesis of Arg 116 has a more dramatic effect on the in vivo stability of PapD (as measured by pulse−chase experiments of PapD production in the periplasm) than mutagenesis of either Glu 83 or Asp 196 (*4*). Future experiments will be aimed at probing in more detail the effect of this salt-bridge as well as other residues on the formation of the domain−domain interface, under conditions where proline isomerization is not rate limiting.

ACKNOWLEDGMENT

We thank Bob Horton for excellent technical assistance and Johnna Roose for initial work on fluorophenylalanine labeling of PapD.

REFERENCES

1. Lindberg, F., Tennent, J. M., Hultgren, S. J., Lund, B., and Normark, S. (1989) PapD, a periplasmic transport protein in P-pilus biogenesis, *J. Bacteriol. 171*, 6052−6058.
2. Holmgren, A., and Branden, C. I. (1989) Crystal structure of chaperone protein PapD reveals an immunoglobulin fold, *Nature 342*, 248−251.
3. Bann, J. G., Pinkner, J., Hultgren, S. J., and Frieden, C. (2002) Real-time and equilibrium (19)F-NMR studies reveal the role of domain-domain interactions in the folding of the chaperone PapD, *Proc. Natl. Acad. Sci. U.S.A. 99*, 709−714.
4. Hung, D. L., Knight, S. D., and Hultgren, S. J. (1999) Probing conserved surfaces on PapD, *Mol. Microbiol. 31*, 773−783.
5. Hoeltzli, S. D., and Frieden, C. (1998) Refolding of [6-19F]-tryptophan-labeled *Escherichia coli* dihydrofolate reductase in the presence of ligand: a stopped-flow NMR spectroscopy study, *Biochemistry 37*, 387−398.
6. Brandts, J. F., Halvorson, H. R., and Brennan, M. (1975) Consideration of the possibility that the slow step in protein denaturation reactions is due to cis−trans isomerism of proline residues, *Biochemistry 14*, 4953−4963.
7. Slonim, L. N., Pinkner, J. S., Branden, C. I., and Hultgren, S. J. (1992) Interactive surface in the PapD chaperone cleft is conserved in pilus chaperone superfamily and essential in subunit recognition and assembly. *EMBO J. 11*, 4747−4756.
8. Fürter, R. (1998) Expansion of the genetic code: site-directed p-fluoro-phenylalanine incorporation in *Escherichia coli*, *Protein Sci. 7*, 419−426.
9. Muchmore, D. C., McIntosh, L. P., Russell, C. B., Anderson, D. E., and Dahlquist, F. W. (1989) Expression and nitrogen-15 labeling of proteins for proton and nitrogen-15 nuclear magnetic resonance, *Methods Enzymol. 177*, 44−73.
10. Hoeltzli, S. D., and Frieden, C. (1995) Stopped-flow NMR spectroscopy: real-time unfolding studies of 6-19F-tryptophan-labeled *Escherichia coli* dihydrofolate reductase, *Proc. Natl. Acad. Sci. U.S.A. 92*, 9318−9322.
11. Hoeltzli, S. D., Ropson, I. J., and Frieden, C. (1994) *Application of Equilibrium and Stopped-Flow 19F NMR Spectroscopy to*

Protein Folding: Studies of E. coli Dihydrofolate Reductase, Vol. V, Academic Press, New York.
12. Santoro, M. M., and Bolen, D. W. (1988) Unfolding free energy changes determined by the linear extrapolation method. 1. Unfolding of phenylmethanesulfonyl α-chymotrypsin using different denaturants, *Biochemistry 27*, 8063−8068.
13. Frieden, C., Hoeltzli, S. D., and Bann, J. G. (2004) The preparation of 19F-labeled proteins for NMR studies, *Methods Enzymol*. *380*, 400−415.
14. Hubbard, S. J., and Thornton, J. M. (1992−1996), *Naccess* V2.1.1.
15. Bretscher, L. E., Jenkins, C. L., Taylor, K. M., DeRider, M. L., and Raines, R. T. (2001) Conformational stability of collagen relies on a stereoelectronic effect, *J. Am. Chem. Soc. 123*, 777−778.
16. Budisa, N., Huber, R., Golbik, R., Minks, C., Weyher, E., and Moroder, L. (1998) Atomic mutations in annexin V−thermodynamic studies of isomorphous protein variants, *Eur. J. Biochem. 253*, 1−9.
17. Minks, C., Huber, R., Moroder, L., and Budisa, N. (1999) Atomic mutations at the single tryptophan residue of human recombinant annexin V: effects on structure, stability, and activity, *Biochemistry 38*, 10649−10659.
18. Reimer, U., Scherer, G., Drewello, M., Kruber, S., Schutkowski, M., and Fischer, G. (1998) Side-chain effects on peptidyl-prolyl cis/trans isomerisation, *J. Mol. Biol. 279*, 449−460.
19. Frieden, C. (2003) The kinetics of side chain stabilization during protein folding, *Biochemistry 42*, 12439−12446.
20. Jacob-Dubuisson, F., Pinkner, J., Xu, Z., Striker, R., Padmanhaban, A., and Hultgren, S. J. (1994) PapD chaperone function in pilus biogenesis depends on oxidant and chaperone-like activities of DsbA, *Proc. Natl. Acad. Sci. U.S.A. 91*, 11552−11556.
21. Hermanns, U., Sebbel, P., Eggli, V., and Glockshuber, R. (2000) Characterization of FimC, a periplasmic assembly factor for biogenesis of type 1 pili in *Escherichia coli*, *Biochemistry 39*, 11564−11570.
22. Bullock, T. L., Roberts, T. M., and Stewart, M. (1996) 2.5 Å resolution crystal structure of the motile major sperm protein (MSP) of *Ascaris suum*, *J. Mol. Biol. 263*, 284−296.
23. Italiano, J. E., Jr., Stewart, M., and Roberts, T. M. (2001) How the assembly dynamics of the nematode major sperm protein generate amoeboid cell motility, *Int. Rev. Cytol. 202*, 1−34.
24. Kline, A. D., Braun, W., and Wüthrich, K. (1988) Determination of the complete three-dimensional structure of the α-amylase inhibitor Tendamistat in aqueous solution by nuclear magnetic resonance and distance geometry, *J. Mol. Biol. 204*, 675−724.
25. Wiegand, G., Epp, O., and Huber, R. (1995) The crystal structure of porcine pancreatic α-amylase in complex with the microbial inhibitor Tendamistat, *J. Mol. Biol. 247*, 99−110.
26. Haaf, A., Butler, P. J., Kent, H. M., Fearnley, I. M., Roberts, T. M., Neuhaus, D., and Stewart, M. (1996) The motile major sperm protein (MSP) from Ascaris suum is a symmetric dimer in solution, *J. Mol. Biol. 260*, 251−260.
27. Toumadje, A., and Johnson, W. C., Jr. (1995) Systemin has the characteristics of a poly(L-proline) II helix, *J. Am. Chem. Soc. 117*, 7023−7024.
28. Visser, L., and Louw, A. I. (1978) The conformations of cardiotoxins and neurotoxins from snake venoms, *Biochim. Biophys. Acta 533*, 80−89.
29. Drake, A. F., Dufton, M. J., and Hider, R. C. (1980) Circular dichroism of elapidae protein toxins, *Eur. J. Biochem. 105*, 623−630.
30. Brandts, J. F., Hu, C. Q., Lin, L. N., and Mos, M. T. (1989) A simple model for proteins with interacting domains. Applications to scanning calorimetry data, *Biochemistry 28*, 8588−8596.
31. Janin, J., and Chothia, C. (1985) Domains in proteins: definitions, location, and structural principles, *Methods Enzymol 115*, 420−430.
32. Janin, J., Miller, S., and Chothia, C. (1988) Surface, subunit interfaces and interior of oligomeric proteins, *J. Mol. Biol. 204*, 155−164.
33. Janin, J., and Chothia, C. (1990) The structure of protein−protein recognition sites, *J. Biol. Chem. 265*, 16027−16030.
34. Holmgren, A., Kuehn, M. J., Branden, C. I., and Hultgren, S. J. (1992) Conserved immunoglobulin-like features in a family of periplasmic pilus chaperones in bacteria, *EMBO J. 11*, 1617−1622.
35. Hung, D. L., Knight, S. D., Woods, R. M., Pinkner, J. S., and Hultgren, S. J. (1996) Molecular basis of two subfamilies of immunoglobulin-like chaperones, *EMBO J. 15*, 3792−3805.

BI048614U